

Filling the gap in the IERS C01 polar motion series in 1858.9–1860.9

Zinovy Malkin¹, Nina Golyandina², Roman Olenev³

¹Pulkovo Observatory, St. Petersburg, 196140, Russia, malkin@gaoran.ru

²Faculty of Mathematics and Mechanics, St. Petersburg State University,
St. Petersburg, 199034, Russia, n.golyandina@spbu.ru

³Faculty of Mathematics and Mechanics, St. Petersburg State University,
St. Petersburg, 199034, Russia, roman.olenov.cs@mail.ru

December 10, 2024

Abstract

The IERS C01 Earth orientation parameters (EOP) series contains the longest reliable record of the Earth’s rotation. In particular, the polar motion (PM) series beginning from 1846 provides a basis for investigation of the long-term PM variations. However, the pole coordinate Y_p in the IERS C01 PM series has a 2-year gap, which makes this series not completely evenly spaced. This paper presents the results of the first attempt to overcome this problem and discusses possible ways to fill this gap. Two novel approaches were considered for this purpose: deterministic astronomical model consisting of the bias and the Chandler and annual wobbles with linearly changing amplitudes, and statistical data-driven model based on the Singular Spectrum Analysis (SSA). Both methods were tested with various options to ensure robust and reliable results. The results obtained by the two methods generally agree within the Y_p errors in the IERS C01 series, but the results obtained by the SSA approach can be considered preferable because it is based on a more complete PM model.

1 Introduction

Time series of the Earth orientation parameters (EOP) are the main source of information for investigation of the Earth’s rotation, in particular the motion of the Earth’s rotation axis in the terrestrial reference frame, which is also called polar motion (PM). The PM is a complex phenomenon, which consists of many variational components including trends and (quasi)periodical oscillations with periods from several hours to several decades. To study slow PM variations, long time series of the pole coordinates X_p and Y_p is needed. The longer the time interval covered by EOP series, the lower frequency variations can be detected and investigated.

The international standard of the EOP series is the combined series computed by the International Earth Rotation and Reference Systems Service (IERS) (Bizouard et al., 2019). The IERS C01 EOP series contains the longest PM series derived from astronomical observations lasting from 1846 to now¹. It is widely used for analysis of the decadal variations in Earth’s rotation (Rykhlova and Kurbasova, 1990; Kołaczek and Kosek, 1999; Gambis, 2000; Yatskiv, 2000; Höpfner, 2004; Guo et al., 2005; Malkin and Mil 2010; Zotov, 2010; Miller, 2011; Seitz et al., 2012; Zotov and Bizouard, 2012; Beutler et al., 2020; Lopes et al., 2022; Zotov et al., 2022; Yamaguchi and Furuya, 2024).

¹<ftp://hpiers.obspm.fr/iers/eop/eopc01/eopc01.iau2000.1846-now>

Table 1: Content of the IERS C01 polar motion series.

Date interval	Data source
1846 – 1889	Rykhlova (1969, 1970)
1890 – 1899	Fedorov et al. (1972)
1900 – 1961	Vondrák et al. (1995, 2010)
1962 – now	Bizouard et al. (2019)

However, the IERS PM series has a 2-year gap in Y_p pole coordinate in the date range 1858.8 to 1861.0. Of course, a time series without missing epochs is always better than a series with a gap. Missing data can cause problems in statistical data analysis. In particular, for spectral analysis, most of the standard methods used require continuous regularly spaced data. If the latter is the case, the results are free from the risk of introducing spurious frequencies in the spectrum. It is also possible to use other efficient analysis methods for regularly spaced data. The reconstructed continuous evenly spaced PM series can also provide new information about the evolution of the Earth’s rotation modes in the gap epochs.

In this paper, for the first time, to our knowledge, we examine possible approaches to address the problem of filling the gap in the IERS C01 series. The challenge is to fill in the missing Y_p values in the series while preserving its structure as much as possible. For this purpose, two methods of analysis were considered. The first is the use of a deterministic astronomical model, specially developed for this study and consisted of three components: bias, Chandler wobble (CW), and annual wobble (AW) (hereafter referred to as BCA model). The second data-driven statistical model has been constructed using the Singular Spectrum Analysis (SSA) (Golyandina et al., 2001).

The paper is organized as follows. Section 2 describes the data used in this study and presents the results of its preliminary analysis. Section 3 is devoted to deriving a deterministic model of the IERS C01 series. A refined analysis of the IERS C01 PM series using the SSA technique is performed in Section 4. Section 5 sums up the results obtained in this work. Concluding remarks on this study are given in the final Section.

2 Data description and preliminary analysis

The IERS C01 PM series consists of several parts as described in Table 1. The epoch step in this series is 0.1 yr in 1846–1890, and 0.05 yr starting with 1890.

In this study, the beginning of the IERS C01 series in the date range 1846 to 1899 was used. It lacks Y_p data from 1858.9 to 1860.9 inclusive. In total, 21 epochs are missing. The middle gap epoch is 1859.9. The PM data used in this work are shown in Fig. 1

Although the polar motion variations described by the IERS C01 series for 1846–1899 are assumed to consist mainly of AW and CW components, possibly with bias², spectral analysis has shown that in fact the signal has a more complex structure as shown in Fig. 2. These normalized Lomb–Scargle periodograms were computed using the algorithm given by Zechmeister and Kürster (2009) after removing the bias in X_p and Y_p series clearly visible in Fig. 1. As expected, the main spectral peaks correspond to the CW and AW oscillations. However, these spectra show that the C01 series cannot be accurately modeled by a simple BCA model, and more refined analysis adequately corresponding to the data is needed. Such an analysis of the IERS C01 series will be presented in Section 4.

²<ftp://hpiers.obspm.fr/iers/eop/eopc01/EOPC01.GUIDE>

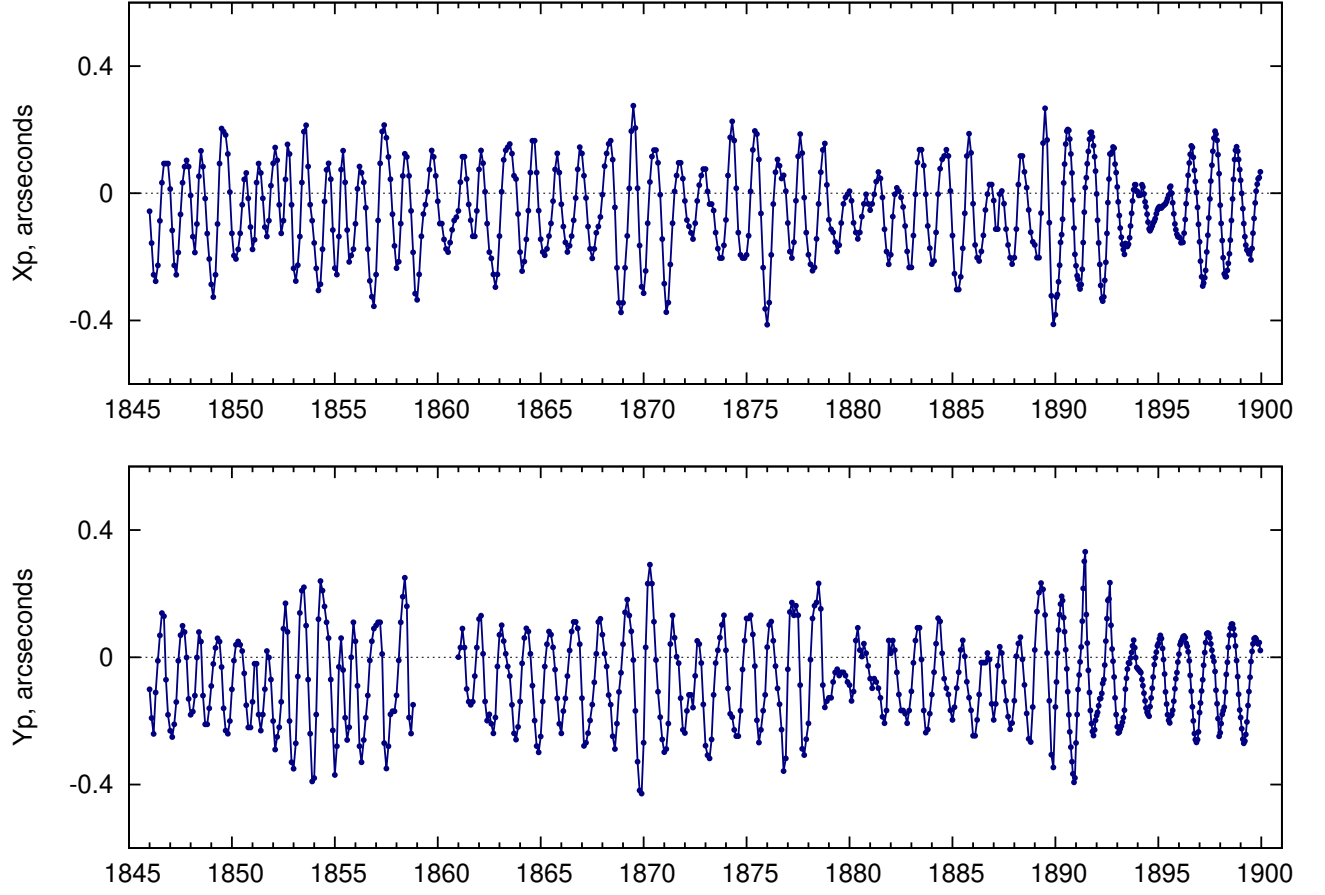


Figure 1: The X_p component (top panel) and Y_p component (bottom panel) of the IERS C01 series.

3 Deterministic model

It is not possible to use a straightforward model consisting of two components, CW and AW, because their amplitudes do not remain constant over time in the date range around the gap (Miller, 2011; Zotov et al., 2022). However, these two independent analyses of the IERS C01 series showed that the CW amplitude grew nearly linearly in 1850–1870. Miller (2011) also showed that the AW amplitude is nearly constant in this period with a tiny increase over time. Therefore, it is possible to construct an approximation model for X_p and Y_p for the period around 1850–1870, consisting of a bias and two oscillations with CW and AW periods and linear amplitude trend:

$$Y_p = a_0 + (1 + a_1^c t) \left(a_c^c \cos \frac{2\pi t}{P_c} + a_s^c \sin \frac{2\pi t}{P_c} \right) + (1 + a_1^a t) \left(a_c^a \cos \frac{2\pi t}{P_a} + a_s^a \sin \frac{2\pi t}{P_a} \right), \quad (1)$$

or, equivalently,

$$\begin{aligned} Y_p = & a_0 + a_{c0}^c \cos \frac{2\pi t}{P_c} + a_{s0}^c \sin \frac{2\pi t}{P_c} + a_{c1}^c t \cos \frac{2\pi t}{P_c} + a_{s1}^c t \sin \frac{2\pi t}{P_c} \\ & + a_{c0}^a \cos \frac{2\pi t}{P_a} + a_{s0}^a \sin \frac{2\pi t}{P_a} + a_{c1}^a t \cos \frac{2\pi t}{P_a} + a_{s1}^a t \sin \frac{2\pi t}{P_a}, \end{aligned} \quad (2)$$

where t is epoch in years (in fact, with respect to the reference epoch), $P_c=1.19$ yr is the period of the CW, and $P_a=1$ yr is the period if the AW.

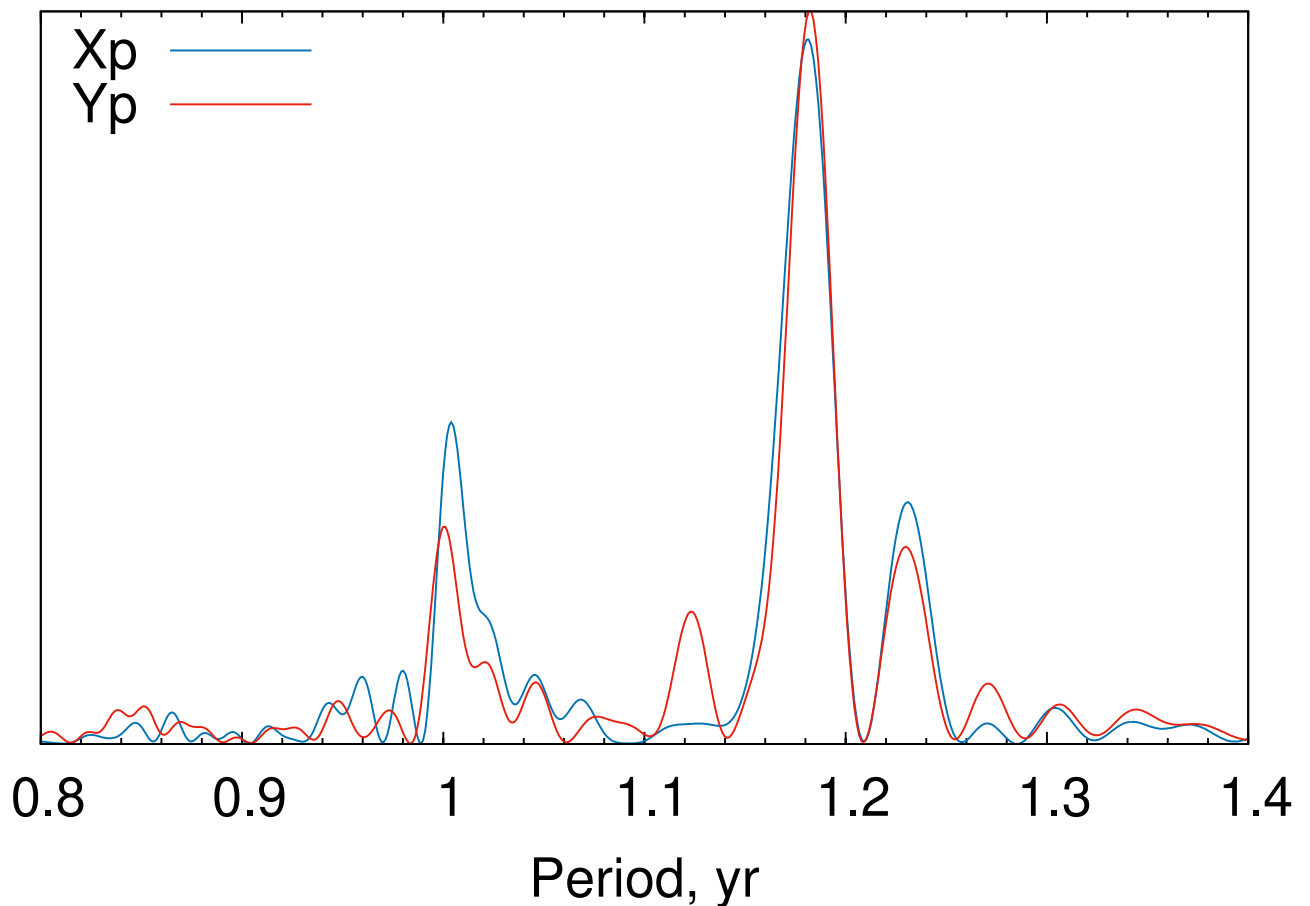


Figure 2: Normalized Lomb-Scargle periodogram of the IERS C01 series for the interval 1846–1899.

The nine parameters of this model were adjusted on seven intervals of length of 12 to 24 years in 2-year increments centered on the middle epoch of the gap in Y_p series, 1859.9. The results of the computation of the filling Y_p values are shown in Fig. 3. The differences between 7 variants are within the error of Y_p in the IERS C01 series around the gap, which is $0.09''$.

Generally speaking, an advanced model can be constructed in a similar way with more complicated behavior of trend, and CW and AW amplitudes (and maybe phases), but such an extension does not look reasonable in our case because there is no data enough to fit a many-parameter model. Therefore, analysis based on the BCA model cannot provide a fully satisfactory solution because it relies on a model that only approximately describes the actual pole motion. However, it may be useful for verification of other models. The more reliable solution to the problem to which this study is aimed will be obtained in the next Section using the data-driven SSA technique.

4 SSA analysis

The SSA method is one of the most powerful tools for analyzing time series with a complex structure (Vautard and Ghil, 1989; Elsner and Tsonis, 1996; Golyandina et al., 2001; Ghil et al., 2002; Golyandina et al., 2018). It is widely used for analyzing geodetic, geophysical, and astronomical time

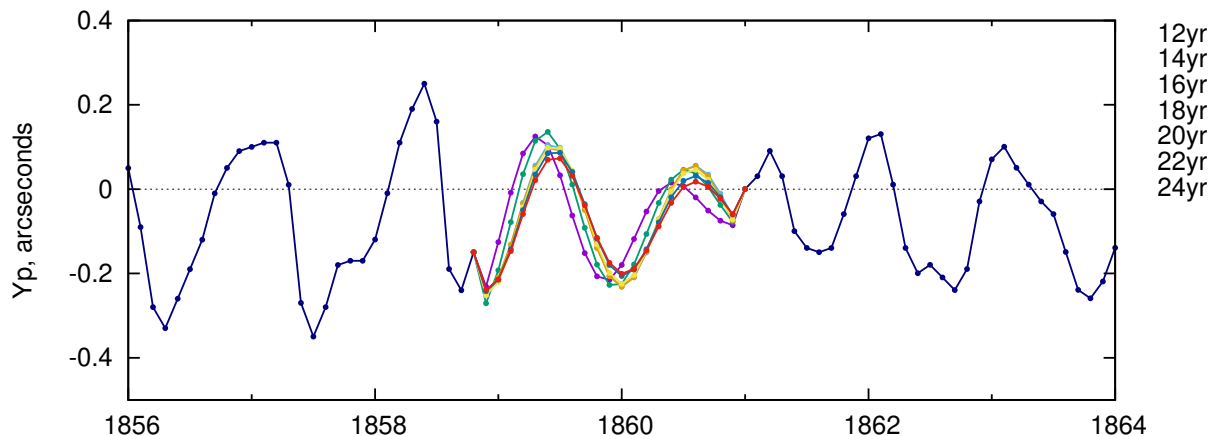


Figure 3: IERS C01 Y_p series with filled missed data between 1858.9 and 1860.9 using the BCA model. Plot titles show date intervals used to fit the Y_p data to the model.

series, in particular, for filling gaps in time series (Konrashov and Ghil, 2006; Golyandina and Osipov, 2007; Shen et al., 2015; Okhotnikov and Golyandina, 2019; Yi and Sneeuw, 2021; Ji et al., 2023).

For the C01 time series, we will consider a model in the form of signal plus noise, where the signal consists of three main components: trend, AW, and CW, with possible addition of other smaller components. Unlike the deterministic BAC model described above, the SSA analysis does not imply a priori restrictions on the trend, AW and CW variations.

We will process time series with 10 measurements per year. Thus, the AW component corresponds to a period of 10 points, and the CW component corresponds to a period of about 11.9 points. For further presentation of our method, we denote IERS C01 PM coordinates X_p and Y_p as X and Y , respectively.

Let us first describe the general approach to gap filling. Suppose there is a method that knows how to remove noise from a noisy signal. Then we can propose a simple iterative gap-filling method. First, the places with missing values are filled with some initial values, e.g., the mean of the series, then the signal extraction is performed, the obtained signal estimates are put at the gaps, the signal extraction method is applied again, and so the procedure is repeated until convergence.

Typically, the signal estimation method has some parameters. Then the approach is as follows. An artificial gap is placed in the part of the series Y that does not contain gaps and the parameters are chosen so that the gap filling error is minimized. For the stability of the result, the error of gap filling is calculated for different locations of gaps and the errors are averaged. It is natural to choose the type of artificial gaps the same as the actual one. For example, if the actual gap consists of consecutive missing values and has length M , then artificial gaps should be the same.

Algorithm 1 (Finding the filling error on artificial gaps):

Input parameters: time series Y with a gap, length M of artificial gap interval, set of intervals with artificial gaps of size R , measure of filling errors.

1. Take an interval of length M from the set of artificial gaps and replace the values of the series Y in this interval by missing values.
2. Fill the artificial gap from step 1 together with the actual one using iterative gap filling.

3. Calculate the error between the values imputed in step 2 for artificial gaps and the actual values of the series Y in the corresponding interval.
4. Repeat steps 1–3 R times for the given set of R intervals of artificial missing values. For each interval, the error is calculated according to step 3.

Result: The arithmetic average of the R errors computed in step 4.

The SSA method in its version for signal extraction has only two parameters, the window length L and the number of components r . At the first stage, the time series $\mathbf{X} = (x_1, \dots, x_N)$ is transformed into the so-called trajectory matrix

$$\mathbf{X} = \begin{pmatrix} x_1 & x_2 & \dots & x_K \\ x_2 & \ddots & \ddots & x_{K+1} \\ \vdots & \ddots & \ddots & \vdots \\ x_L & x_{L+1} & \dots & x_N \end{pmatrix} \quad (3)$$

using the parameter L . Next, the singular value decomposition (SVD) of the trajectory matrix is constructed. Let $\mathbf{S} = \mathbf{X}\mathbf{X}^T$, $\lambda_1, \dots, \lambda_L$ be the eigenvalues of the matrix \mathbf{S} taken in non-decreasing order, U_1, \dots, U_L be the orthonormalized system of eigenvectors corresponding to these eigenvalues. Let $d = \max\{k : \lambda_k > 0\}$ and $V_k = \mathbf{X}^T U_k / \sqrt{\lambda_k}$, $k = 1, \dots, d$. Then the SVD of the matrix \mathbf{X} can be represented as a sum of elementary matrices

$$\mathbf{X} = \mathbf{X}_1 + \dots + \mathbf{X}_d, \quad (4)$$

where $\mathbf{X}_k = \sqrt{\lambda_k} U_k V_k^T$, $k = 1, \dots, d$.

In the second step, the first r of the elementary matrices of the SVD are summed:

$$\mathbf{Y} = \mathbf{X}_1 + \dots + \mathbf{X}_r, \quad (5)$$

and their sum is converted into a time series.

$$\tilde{y}_s = \sum_{(l,k) \in A_s} y_{lk} / |A_s|, \quad (6)$$

where y_{lk} are the elements of the matrix \mathbf{Y} , the sets $A_s = \{(l, k) : l + k = s + 1, 1 \leq l \leq L, 1 \leq k \leq K\}$, $s = 1, \dots, N$, give the indices corresponding to the elements on the side diagonals, $|A_s|$ denotes the number of elements in the sets A_s .

In the real form, the SSA method works well with signals as a sum of possibly modulated harmonics (Golyandina et al., 2001). Such a modification of SSA applied to a single time series Y will be called hereafter 1D-SSA.

It was shown in Golyandina et al. (2015) that if several signals have the same periods (with the same modulation), the Multivariate SSA (MSSA), a generalization of SSA for time series system analysis, extracts the signal more accurately. Such a method allows us to process \mathbf{X} and \mathbf{Y} series together.

Taking into account the physical nature of the pole coordinates, this looks reasonable to consider a representation of the PM series as a complex time series. If the input signal consists of two harmonics with a phase shift of $\pi/2$, then the generalization of SSA for the analysis of complex time series extracts

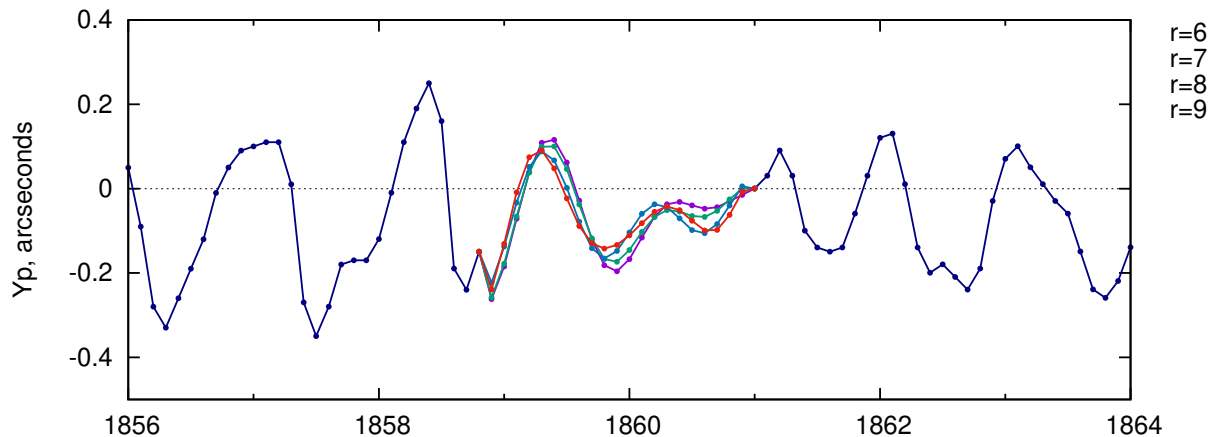


Figure 4: IERS C01 Y_p series with filled missed data between 1858.9 and 1860.9 computed using the CSSA model with $L=119$ and r from 6 to 9.

the signal even more accurately (Golyandina et al., 2015). In the case of Complex SSA (CSSA) for a time series of the form $x_n + iy_n$, $n = 1, \dots, N$, the transpose operator T is replaced by the Hermite conjugate operator H . The complex form of SSA has been considered since its origin. In the complex form, the first descriptions of the method can be found, for example, in Kumaresan and Tufts (1982); Kepenne and Lall (1996).

To ensure more reliable results, we considered the three methods described above for reconstruction of PM signal: basic 1D-SSA for the series Y , MSSA for the series (X, Y) , and CSSA for the series $X + iY$.

An important option for a practical SSA realization is a choice of the window length. Recommendations for optimal window selection include proportionality to the periods of the harmonics we want to extract (Golyandina et al., 2001). Therefore, for the window length L we will consider two values, 119 and 238 points, since the AW and CW periods (10 and about 11.9, respectively) are included near integer number of times in windows of this length.

The parameter that we want to optimize using artificial gaps is r , the number of the SVD components assigned to the signal. We will call r the model order. To find the optimal value of the model order, we vary it from 1 to 17 and calculate the error of gap filling according to Algorithm 1. We used the root-mean-square error (RMSE) and the mean absolute error (MAE) as a measure of the difference between the imputed values and the input time series values.

As a set of artificial gaps, we considered $R = 120$ gap intervals of length $M = 21$, the same as the actual gap. The first interval starts at 1846.1, the remaining 119 intervals are obtained by successively shifting the initial interval four points forward (intervals with actual gaps were excluded).

The mean MAE and RMSE errors for these models are presented in Table 2. These test results have shown that the most precise filling of artificial gaps were achieved using CSSA with $L=119$ and r from 6 to 9. Similar results were obtained for RMSE, for which models of the same orders showed somewhat larger errors overall, but the optimal parameters r and L turned out to be the same as for the MAE error estimate. Thus, it has been found that the obtained results do not depend on the choice of the method for estimating the modeling error.

The gap-filling plots with the best parameters (CSSA, $L=119$, $r = 6 \dots 9$) are shown in Fig. 4.

Consider the CSSA decomposition components of the time series Y after filling the actual gap. Recall that the imaginary parts of the complex components are related to the series Y . The latter for the CSSA 6-component solution with $L = 119$ are shown in Fig. 5, and Fig. 6 shows the Y components

Table 2: MAE/RMSE filling errors (arcseconds) on artificial gaps for SSA model order $r = 1 \dots 17$.

r	$L=119$			$L=238$		
	1D-SSA	MSSA	CSSA	1D-SSA	MSSA	CSSA
1	0.121/0.143	0.114/0.142	0.104/0.130	0.121/0.143	0.114/0.142	0.106/0.135
2	0.104/0.129	0.109/0.137	0.084/0.110	0.107/0.134	0.108/0.137	0.087/0.115
3	0.089/0.116	0.094/0.118	0.076/0.099	0.091/0.120	0.091/0.118	0.080/0.105
4	0.082/0.109	0.090/0.113	0.072/0.094	0.085/0.113	0.086/0.112	0.076/0.099
5	0.085/0.110	0.092/0.114	0.070/0.090	0.086/0.112	0.086/0.111	0.072/0.094
6	0.083/0.108	0.095/0.117	0.065/0.084	0.083/0.106	0.086/0.109	0.071/0.091
7	0.085/0.111	0.101/0.123	0.064/0.084	0.084/0.106	0.087/0.109	0.066/0.085
8	0.086/0.112	0.106/0.129	0.064/0.084	0.083/0.106	0.090/0.112	0.073/0.093
9	0.090/0.117	0.113/0.137	0.065/0.085	0.084/0.109	0.096/0.118	0.075/0.096
10	0.088/0.113	0.116/0.139	0.068/0.090	0.085/0.109	0.100/0.122	0.076/0.097
11	0.088/0.111	0.118/0.143	0.071/0.092	0.085/0.110	0.104/0.126	0.074/0.094
12	0.080/0.102	0.123/0.149	0.072/0.095	0.083/0.107	0.105/0.127	0.074/0.095
13	0.081/0.106	0.129/0.156	0.073/0.097	0.084/0.108	0.108/0.130	0.076/0.098
14	0.085/0.111	0.133/0.160	0.073/0.099	0.085/0.108	0.110/0.133	0.076/0.099
15	0.090/0.118	0.137/0.166	0.071/0.097	0.090/0.114	0.114/0.137	0.070/0.091
16	0.093/0.121	0.140/0.169	0.075/0.102	0.086/0.110	0.116/0.139	0.070/0.091
17	0.092/0.122	0.143/0.173	0.081/0.108	0.088/0.115	0.119/0.142	0.070/0.091

for the 9-component CSSA solution.

It can be seen the leading six components of the 9-component solution have practically the same periods as those for the 6-component solution. Some components show two spectral peaks, which can be caused by mixing of two periodicities or by phase instability of the component. In all solutions, the first component corresponds to the main CW oscillation, and the third component corresponds to the main AW oscillation.

Since the imputed values for the model orders r from 6 to 9 (CSSA with $L = 119$) provide approximately equal errors on the artificial gaps, the average of these values can be recommended as the final method of filling in the actual gap in the IERS C01 series. This filling method has a slightly smaller error (0.063 vs. 0.064–0.065) and a bit smaller error variation (standard deviation) (0.0251 vs 0.0252–0.0265) on the considered set of artificial gaps, in comparison with gap filling by r components separately.

5 Final results

Average results (filling Y_p values) computed by the BCA and SSA methods are presented in Table 3 with the precision corresponding to the IERS C01 series. The fourth column of Table 3 contains the differences between the results obtained by two methods, and the last column contains the average of the results obtained by two methods. The IERS C01 series with added filling values is shown in Fig. 7.

A better agreement between the two methods can be seen in the first year of the gap interval, 1859–1860. The agreement in the second year of the interval, 1860–1861, is somewhat worse, but can be considered satisfactory, considering that the Y_p error in the IERS C01 series is $0.09''$. Generally

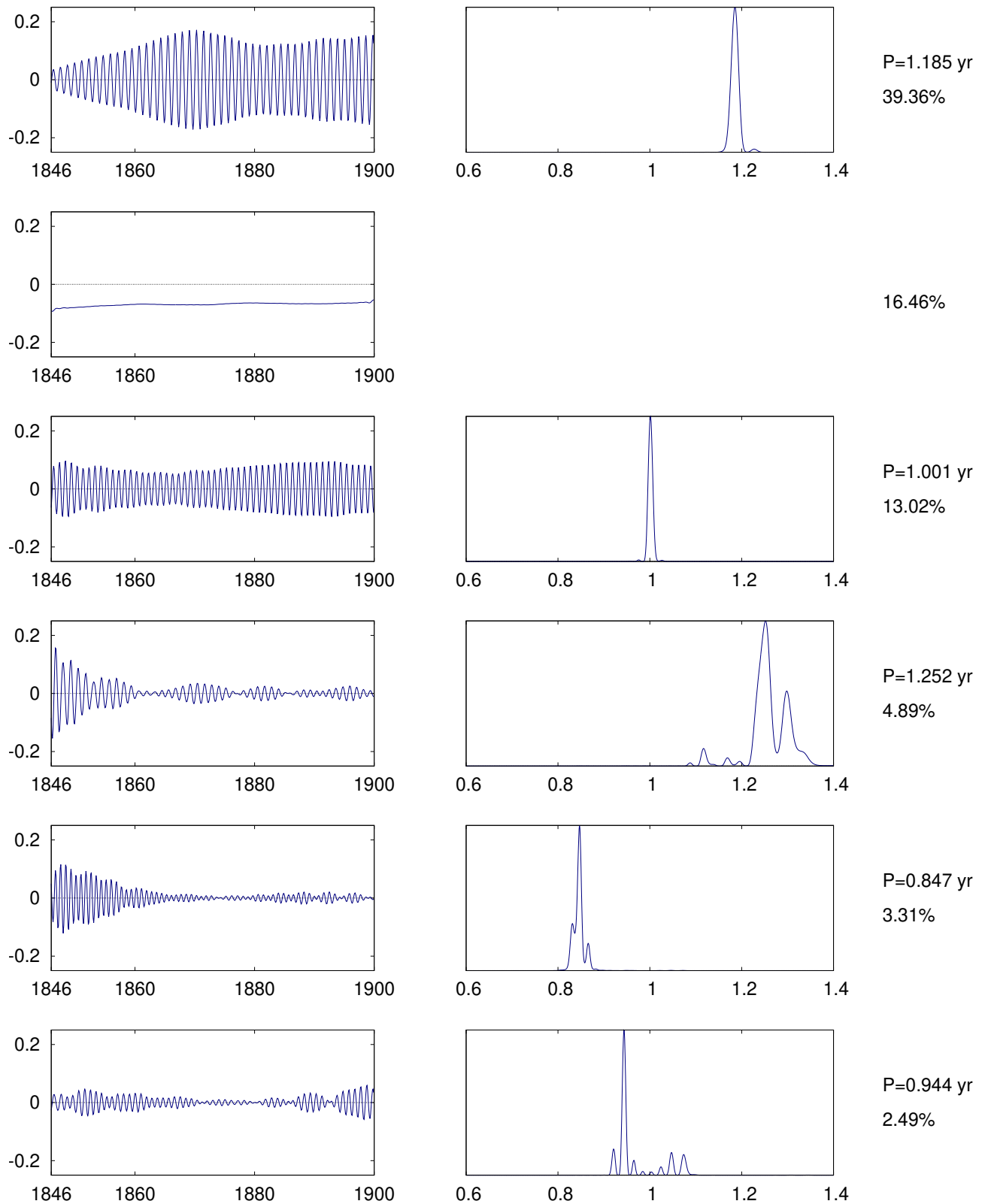


Figure 5: The Y components of CSSA solution with $r=6$ (in arcseconds) and their normalized spectra. The period of the most powerful oscillation and the contribution of the component to the total signal are shown on the right.

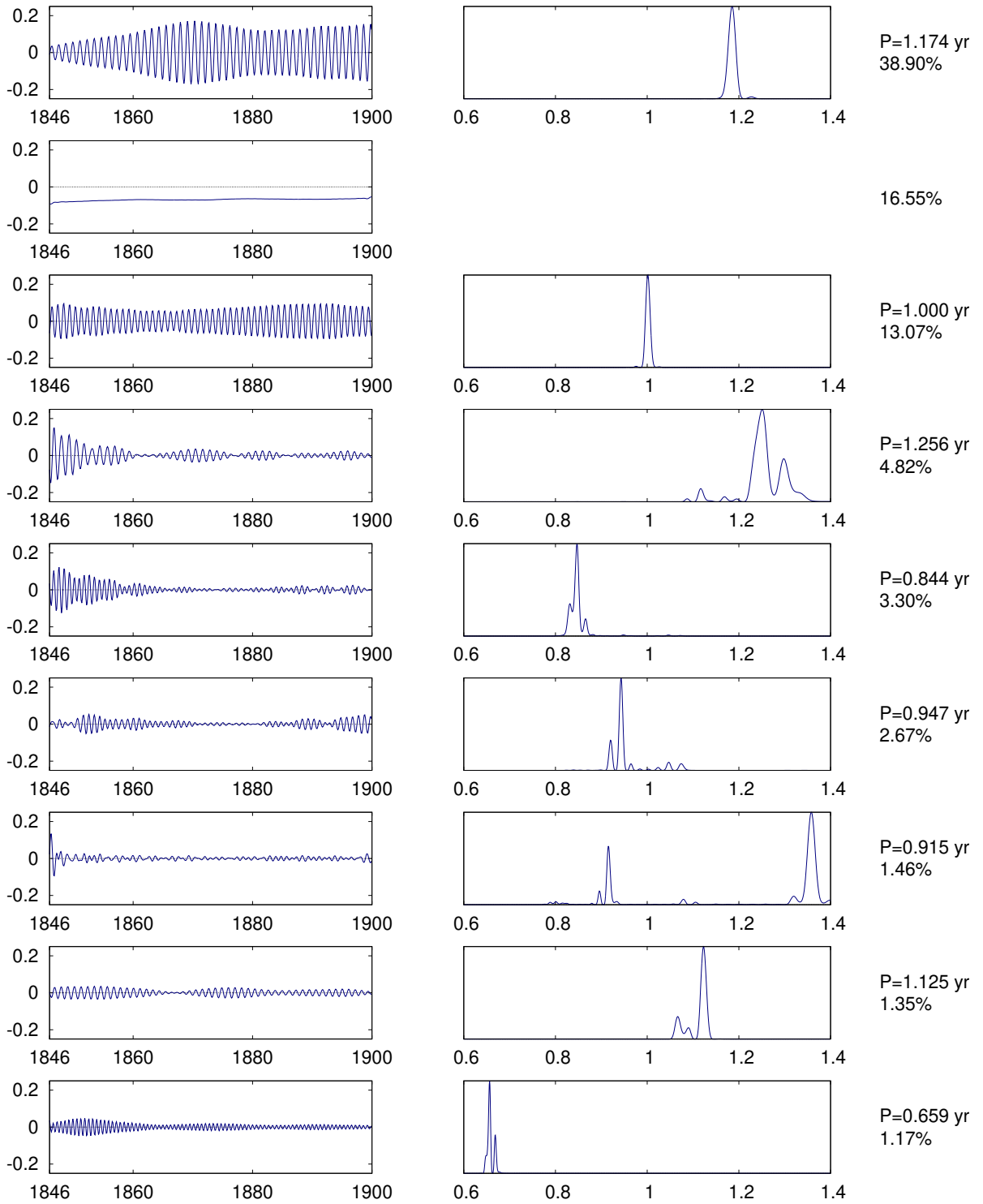


Figure 6: The Y components of CSSA solution with $r=9$ (in arcseconds) and their normalized spectra. The period of the most powerful oscillation and the contribution of the component to the total signal are shown on the right.

Table 3: Filled Y_p values, arcseconds.

Epoch	Model		Difference	Average
	BCA	SSA	BCA-SSA	
1858.9	-0.24731	-0.24542	-0.00189	-0.24636
1859.0	-0.19886	-0.15757	-0.04129	-0.17822
1859.1	-0.11187	-0.04478	-0.06708	-0.07833
1859.2	-0.01403	0.05086	-0.06489	0.01841
1859.3	0.06414	0.09691	-0.03278	0.08053
1859.4	0.09921	0.08292	0.01628	0.09106
1859.5	0.08210	0.02188	0.06022	0.05199
1859.6	0.02039	-0.05820	0.07859	-0.01890
1859.7	-0.06490	-0.12716	0.06226	-0.09603
1859.8	-0.14678	-0.16397	0.01719	-0.15537
1859.9	-0.20112	-0.16264	-0.03847	-0.18188
1860.0	-0.21406	-0.13195	-0.08211	-0.17300
1860.1	-0.18546	-0.09002	-0.09543	-0.13774
1860.2	-0.12761	-0.05632	-0.07129	-0.09197
1860.3	-0.06015	-0.04340	-0.01675	-0.05178
1860.4	-0.00312	-0.05167	0.04855	-0.02740
1860.5	0.02922	-0.06956	0.09878	-0.02017
1860.6	0.03183	-0.07982	0.11165	-0.02399
1860.7	0.00889	-0.06961	0.07851	-0.03036
1860.8	-0.02926	-0.03929	0.01003	-0.03427
1860.9	-0.07053	-0.00424	-0.06628	-0.03739

speaking, it should be kept in mind that the accuracy of the reconstruction is limited by the accuracy of the IERS C01 data, especially before the gap in the 1840s and 1850s.

6 Conclusions

In this paper, the first attempt was made to address the problem of filling the 2-year gap in the IERS C01 Y_p series in 1858.9–1860.9. Two methods were proposed and investigated for this purpose. The first is LS adjustment of the BCA model consisting of a bias and CW and AW harmonics with linearly changing amplitude. In a general case, such a model can be extended to more complicated trend and amplitude variations. The second is SSA for complex PM data, or CSSA, which allows us to get a fully data-driven solution not limited to the parameters of the deterministic BCA model.

We consider the result obtained by SSA as more reliable because it takes into account all the features of the observed PM data and all the main components of its structure, while the deterministic model uses only predefined components, which may not adequately describe the results of the observations. However, we present both the results obtained by the BCA and SSA methods in Table 3 so that the user can choose the variant that looks most appropriate for the problem under investigation, or simply use the average of the two.

Incorporating the proposed fill values into the IERS C01 series would provide continuous, evenly

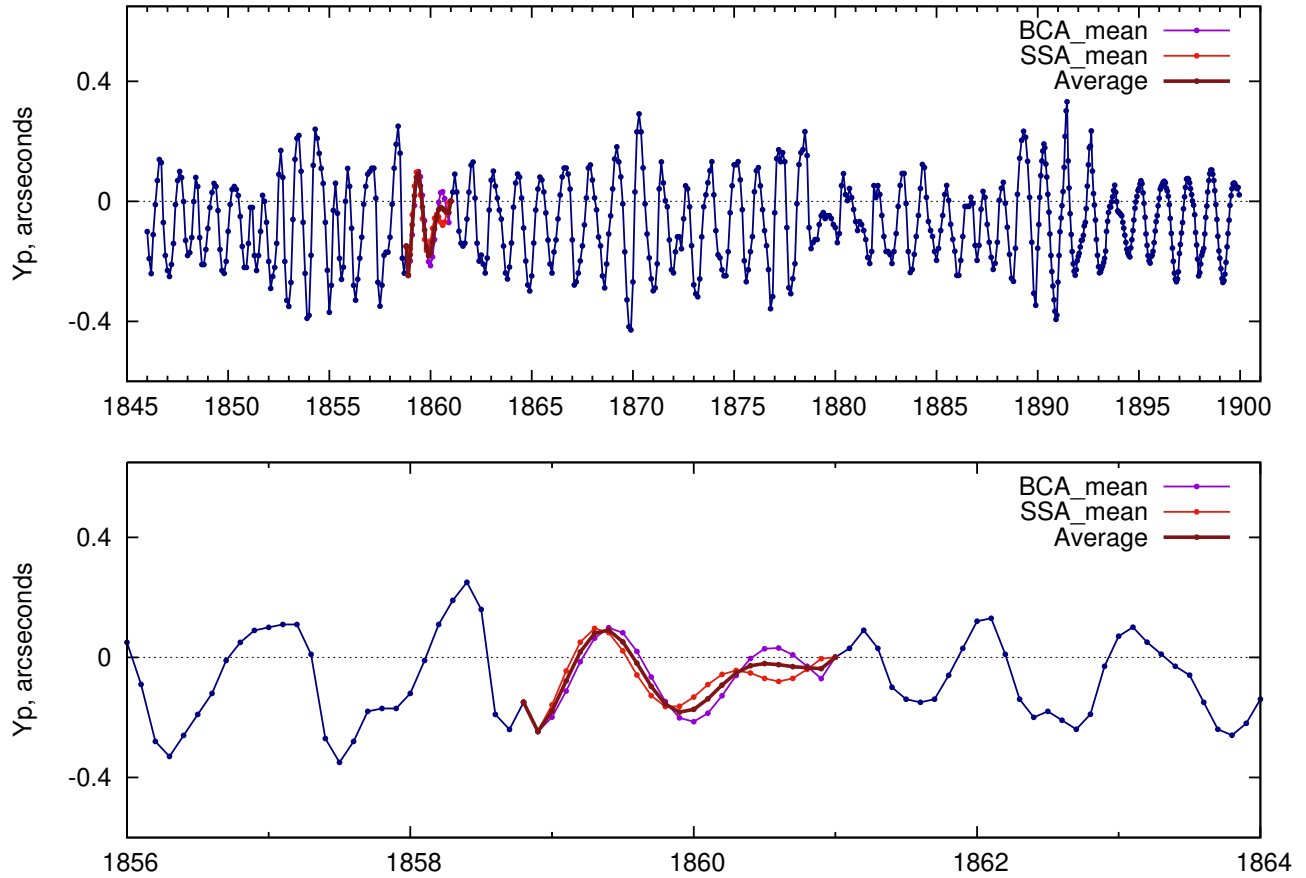


Figure 7: IERS C01 Y_p series with filled missed data between 1858.9 and 1860.9 using the average values for both BCA and SSA models.

spaced series over the entire date range. This will allow for faster and more accurate analysis methods for PM analysis and mitigate a bias in PM modeling caused by the uneven spacing of the original IERS C01 series.

Acknowledgments

The SSA data analysis was performed using the package `Rssa`, <https://CRAN.R-project.org/package=Rssa>. This research has made use of SAO/NASA Astrophysics Data System (ADS), <https://ui.adsabs.harvard.edu>. The figures were prepared using `gnuplot`, <http://www.gnuplot.info/>.

References

Beutler G, Villiger A, Dach R, Verdun A, Jäggi A (2020) Long polar motion series: Facts and insights. *Advances in Space Research* 66(11):2487–2515. <https://doi.org/10.1016/j.asr.2020.08.033>

- Bizouard C, Lambert S, Gattano C, Becker O, Richard JY (2019) The IERS EOP 14C04 solution for Earth orientation parameters consistent with ITRF 2014. *Journal of Geodesy* 93(5):621–633. <https://doi.org/10.1007/s00190-018-1186-3>
- Elsner JB, Tsonis AA (1996) *Singular Spectrum Analysis: A New Tool in Time Series Analysis*. Springer
- Fedorov EP, Korsun' AA, Major SP, Panchenko NI, Taradij VK, Yatskiv YS (1972) Motion of the Earth's pole from 1890.0 to 1969.0. *Kyiv, Naukova Dumka*
- Gambis D (2000) Long-term Earth Orientation Monitoring Using Various Techniques. In: Dick S, McCarthy D, Luzum B (eds) *IAU Colloq. 178: Polar Motion: Historical and Scientific Problems*, *Astronomical Society of the Pacific Conference Series*, vol 208, p 337
- Ghil M, Allen MR, Dettinger MD, Ide K, Kondrashov D, Mann ME, Robertson AW, Saunders A, Tian Y, Varadi F, Yiou P (2002) *Advanced Spectral Methods for Climatic Time Series*. *Reviews of Geophysics* 40(1):1003. <https://doi.org/10.1029/2000RG000092>
- Golyandina N, Osipov E (2007) The “Caterpillar”–SSA method for analysis of time series with missing values. *J Stat Plan Inference* 137(8):2642–2653. <https://doi.org/10.1016/j.jspi.2006.05.014>
- Golyandina N, Nekrutkin V, Zhigljavsky A (2001) *Analysis of Time Series Structure: SSA and related techniques*. Chapman and Hall/CRC (Second edition: Springer, 2020)
- Golyandina N, Korobeynikov A, Shlemov A, Usevich K (2015) Multivariate and 2D Extensions of Singular Spectrum Analysis with the Rssa Package. *J Stat Softw* 67(2):1–78. <https://doi.org/10.18637/jss.v067.i02>
- Golyandina N, Korobeynikov A, Zhigljavsky A (2018) *Singular Spectrum Analysis with R*. Springer, <https://doi.org/10.1007/978-3-662-57380-8>
- Guo JY, Greiner-Mai H, Ballani L, Jochmann H, Shum CK (2005) On the double-peak spectrum of the Chandler wobble. *Journal of Geodesy* 78(11-12):654–659. <https://doi.org/10.1007/s00190-004-0431-0>
- Höpfner J (2004) Low-Frequency Variations, Chandler and Annual Wobbles of Polar Motion as Observed Over One Century. *Surveys in Geophysics* 25(1):1–54. <https://doi.org/10.1023/B:GEOP.0000015345.88410.36>
- Ji K, Shen Y, Chen Q, Wang F (2023) Extended singular spectrum analysis for processing incomplete heterogeneous geodetic time series. *Journal of Geodesy* 97(8):74. <https://doi.org/10.1007/s00190-023-01764-8>
- Keppenne C, Lall U (1996) Complex singular spectrum analysis and multivariate adaptive regression splines applied to forecasting the southern oscillation. *Experimental Long-Lead Bulletin* 5(3):39–40
- Kołaczek B, Kosek W (1999) Variations of the amplitude of the Chandler wobble. In: *Journées 1998 “Systèmes de Référence Spatio-Temporels: Conceptual, Conventional and Practical Studies Related to Earth Rotation”*, pp 215–220

- Kondrashov D, Ghil M (2006) Spatio-temporal filling of missing points in geophysical data sets. *Nonlinear Processes in Geophysics* 13(2):151–159. <https://doi.org/10.5194/npg-13-151-2006>
- Kumaresan R, Tufts D (1982) Estimating the parameters of exponentially damped sinusoids and pole-zero modeling in noise. *IEEE Trans Acoust* 30(6):833–840
- Lopes F, Courtillot V, Gibert D, Le Mouél JL (2022) Extending the Range of Milankovic Cycles and Resulting Global Temperature Variations to Shorter Periods (1–100 Year Range). *Geosciences* 12(12):448. <https://doi.org/10.3390/geosciences12120448>
- Malkin Z, Miller N (2010) Chandler wobble: two more large phase jumps revealed. *Earth, Planets and Space* 62(12):943–947. <https://doi.org/10.5047/eps.2010.11.002>
- Miller NO (2011) Chandler wobble in variations of the Pulkovo latitude for 170 years. *Solar System Research* 45(4):342–353. <https://doi.org/10.1134/S0038094611040058>
- Okhotnikov G, Golyandina N (2019) EOP time series prediction using singular spectrum analysis. In: Corpetti T, Ienco D, Interdonato R, et al (eds) *Proceedings of MACLEAN: MACHine Learning for EArth ObservatioN Workshop*, RWTH Aachen University, Germany, *CEUR Workshop Proceedings*, Vol. 2466
- Rykhlova LV (1969) Motion of the Earth’s Pole, 1846.0-1891.5, from Observations at Pulkovo, Greenwich, and Washington. *Soviet Ast* 12:898
- Rykhlova LV (1970) The coordinates of the Earth’s pole for the years 1846.0-1891.5. *Soobshcheniya Gosudarstvennogo Astronomicheskogo Instituta, Moscow State University* 163:3–10
- Rykhlova LV, Kurbasova GS (1990) The Study of the Structure of 142-Year Series of Pole Coordinates. In: Lieske JH, Abalakin VK (eds) *Inertial Coordinate System on the Sky*, vol 141, p 157
- Seitz F, Kirschner S, Neubersch D (2012) Determination of the Earth’s pole tide Love number k_2 from observations of polar motion using an adaptive Kalman filter approach. *Journal of Geophysical Research (Solid Earth)* 117(B9):B09403. <https://doi.org/10.1029/2012JB009296>
- Shen Y, Peng F, Li B (2015) Improved singular spectrum analysis for time series with missing data. *Nonlinear Processes in Geophysics* 22(4):371–376. <https://doi.org/10.5194/npg-22-371-201510.5194/npgd-1-1947-2014>
- Vautard R, Ghil M (1989) Singular spectrum analysis in nonlinear dynamics, with applications to paleoclimatic time series. *Physica D Nonlinear Phenomena* 35:395–424. [https://doi.org/10.1016/0167-2789\(89\)90077-8](https://doi.org/10.1016/0167-2789(89)90077-8)
- Vondrák J, Ron C, Pešek I, Čepek A (1995) New global solution of Earth orientation parameters from optical astrometry in 1900-1990. *A&A* 297:899–906
- Vondrák J, Ron C, Štefka A (2010) Earth orientation parameters based on EOC-4 astrometric catalog. *Acta Geodyn Geomater* 7(3):245–251
- Yamaguchi R, Furuya M (2024) Can we explain the post-2015 absence of the Chandler wobble? *Earth, Planets and Space* 76(1):1. <https://doi.org/10.1186/s40623-023-01944-y>

- Yatskiv Y (2000) Chandler Motion Observations. In: Dick S, McCarthy D, Luzum B (eds) IAU Colloq. 178: Polar Motion: Historical and Scientific Problems, Astronomical Society of the Pacific Conference Series, vol 208, p 383
- Yi S, Sneeuw N (2021) Filling the Data Gaps Within GRACE Missions Using Singular Spectrum Analysis. *Journal of Geophysical Research (Solid Earth)* 126(5):e2020JB021227. <https://doi.org/10.1029/2020JB021227>
- Zechmeister M, Kürster M (2009) The generalised Lomb-Scargle periodogram. A new formalism for the floating-mean and Keplerian periodograms. *A&A* 496(2):577–584. <https://doi.org/10.1051/0004-6361:200811296>
- Zotov L, Bizouard C (2012) On modulations of the Chandler wobble excitation. *Journal of Geodynamics* 62:30–34. <https://doi.org/10.1016/j.jog.2012.03.010>
- Zotov LV (2010) Dynamical Modeling and Excitation Reconstruction as Fundamental of Earth Rotation Prediction. *Artificial Satellites* 45(2):95–106. <https://doi.org/10.2478/v10018-010-0010-y>
- Zotov LV, Sidorenkov NS, Bizouard C (2022) Anomalies of the Chandler Wobble in 2010s. *Moscow University Physics Bulletin* 77(3):555–563. <https://doi.org/10.3103/S0027134922030134>